

Identification of two glioblastoma-associated stromal cell subtypes with different carcinogenic properties in histologically normal surgical margins

Anne Clavreul · Amandine Etcheverry · Clément Tétaud · Audrey Rousseau · Tony Avril · Cécile Henry · Jean Mosser · Philippe Menei

Received: 22 July 2014 / Accepted: 4 December 2014 / Published online: 13 December 2014
© Springer Science+Business Media New York 2014

Abstract Glioblastoma (GB) is a highly infiltrative tumor recurring within a few centimeters of the resection cavity in 85 % of cases, even in cases of complete tumor resection and adjuvant chemo/radiotherapy. We recently isolated GB-associated stromal cells (GASCs) from the GB peritumoral zone, with phenotypic and functional properties similar to those of the cancer-associated fibroblasts present in the stroma of carcinomas. In particular, GASCs promote blood vessel development and have tumor-promoting effects on glioma cells in vitro and in vivo. In this study, we characterized these cells further, by analyzing the transcriptome and methylome of 14 GASC and five control stromal cell preparations derived from non-GB peripheral

brain tissues. We identified two subtypes of GASCs in surgical margins in GB patients: GASC-A and GASC-B. GASC-B promoted the development of tumors and endothelium, whereas GASC-A did not. A difference in DNA methylation may underlie these two subtypes. We identified various proteins as being produced in the procarcinogenic GASC-B. Some of these proteins may serve as prognostic factors for GB and/or targets for anti-glioma treatment. In conclusion, in this era of personalized therapy, the status of GASCs in GB-free surgical margins should be taken into account, to improve treatment and the prevention of recurrence.

Keywords Translational study · Glioblastoma · Peritumoral brain zone · Cancer-associated fibroblasts

Electronic supplementary material The online version of this article (doi:10.1007/s11060-014-1683-z) contains supplementary material, which is available to authorized users.

A. Clavreul · C. Tétaud · A. Rousseau · P. Menei
LUNAM, Université d'Angers, 49035 Angers, France

A. Clavreul · C. Tétaud · A. Rousseau · P. Menei
INSERM U1066, Micro et Nanomédecines Biomimétiques (MINT), 49933 Angers, France

A. Clavreul · P. Menei
Département de Neurochirurgie, CHU, 49933 Angers, France

A. Clavreul (✉)
INSERM U1066, 49100 Angers, France
e-mail: anne.clavreul@univ-angers.fr

A. Etcheverry · J. Mosser
CNRS, UMR 6290, Institut de Génétique et Développement de Rennes (IGdR), 35043 Rennes, France

A. Etcheverry · J. Mosser
Université Rennes1, UEB, UMS 3480 Biosit, Faculté de Médecine, 35043 Rennes, France

A. Etcheverry · J. Mosser
Service de Génétique Moléculaire et Génomique, CHU Rennes, 35033 Rennes, France

A. Rousseau
Laboratoire Pathologie Cellulaire et Tissulaire, CHU, 49933 Angers, France

T. Avril
Centre Régional de Lutte Contre le Cancer Eugène Marquis, 35000 Rennes, France

C. Henry
Centre Régional de Lutte Contre le Cancer Paul Papin, INSERM U892, 49000 Angers, France

J. Mosser
Plate-forme Génomique Santé Biosit, Université Rennes1, 35043 Rennes, France

Abbreviations

CAFs	Cancer-associated fibroblasts
CM	Conditioned medium
DMEM-HG	Dulbecco's modified Eagles' medium—high glucose
EBM-2	Endothelial basal medium-2
EGM-2	Endothelial cell growth medium-2
FCA	Absolute fold-change
FCS	Foetal calf serum
GASCs	Glioblastoma-associated stromal cells
GB	Glioblastoma
HABS	Human AB serum
HUVECs	Human umbilical vein endothelial cells
PDGFR β	Platelet derived growth factor receptor-beta
α SMA	Alpha smooth muscle actin

Introduction

Glioblastoma (GB) has a poor prognosis, despite aggressive treatment by surgery, radiotherapy and chemotherapy [1, 2]. Even in cases of complete resection of the gadolinium-enhanced portion of the GB, 85 % of recurrences occur in the resection margin [3]. Recurrence is thought to result from the proliferation of residual unresected tumor cells. Such cells have been isolated and shown to display alterations different from those of cells isolated from the corresponding tumor mass [4, 5]. In addition to containing unresected tumor cells, the tumor microenvironment may play a determinant role in local recurrence. It contains a number of different cellular elements, including inflammatory cells, endothelial cells and fibroblasts. Cancer-associated fibroblasts (CAFs), commonly referred to as myofibroblasts, constitute a significant component of the tumor stroma of carcinomas [6]. These cells have been shown to play an active role in reciprocal communication with tumor cells, thereby accelerating tumor growth and progression. We isolated a population of such stromal cells from the histologically normal surgical margins of GB by computer-guided stereotaxic biopsy and primary culture. We named these cells GB-associated stromal cells (GASCs). These cells were mostly located close to blood vessels. They were diploid, did not display the genomic alterations typical of GB cells and expressed markers associated with CAFs, including alpha-smooth muscle actin (α SMA), platelet-derived growth factor receptor-beta (PDGFR β /CD140b) and FSP1/S100A4 [7, 8]. GASCs were also found to have tumor-promoting effects on glioma cells in vitro and in vivo and to have angiogenic properties [7, 8]. All these data suggest that GASCs may be a component of the vascular niche in surgical margins, establishing a

permissive environment for angiogenesis and the proliferation of recurrence-initiating cells.

In this study, we investigated the transcriptomes and methylomes of 14 GASC and five control stromal cell preparations derived from non-GB peripheral brain tissues. We identified two types of GASCs in surgical margins in GB patients: one subtype with, and the other without tumor-promoting and angiogenic properties.

Materials and methods

Establishment of primary GASCs and control stromal cells

The entire project was approved by the local institutional review board (CPP Ouest II) and the *Direction générale de la santé* (DGS). All patients undergoing surgery signed an informed consent form for participation in this study. Peripheral brain biopsy specimens were obtained from 14 patients with de novo GB and from five non-GB patients, for the propagation of primary GASCs and control stromal cells, respectively (Supplementary Table 1). Briefly, biopsy specimens were minced and mechanically dissociated in Dulbecco's modified Eagles' medium—high glucose (DMEM-HG) (Lonza, Verviers, Belgium), as previously described [8]. The resulting suspension was used to seed T80 flasks (Nunc, Dominique Dutsher, Brumath, France) containing DMEM supplemented with 10 % human AB serum (HABS) (EFS, Lyon, France) and 1 % antibiotics (Sigma-Aldrich, Saint Quentin Fallavier, France), which was then incubated at 37 °C in a humidified incubator, under an atmosphere containing 5 % CO₂. After several days, the outgrowth of spindle-shaped cells was observed. Experiments were performed with cells between passages five and seven. GASCs and control stromal cells were diploid, negative for the endothelial marker CD31 and the hematopoietic lineage markers (CD45, CD34), but positive for CAF-associated biomarkers, including α SMA, PDGFR β and FSP1/S100A4 (data not shown).

Cell-line culture

The aneuploid non-tumorigenic (A172) and diploid tumorigenic (U87MG) GB cell lines were provided by ATCC (LGC Promochem, Molsheim, France). They were maintained in the same medium as GASCs and control stromal cells at 37 °C, under an atmosphere containing 5 % CO₂, until they reached 80–90 % confluence.

Human umbilical vein endothelial cells (HUVECs) were purchased from Lonza. Cells were cultured according to the supplier's instructions, in endothelial cell growth medium-2 (EGM-2), corresponding to endothelial basal

medium-2 (EBM-2) containing the supplements and growth factors of the EGM-2 SingleQuot kit (Lonza), in a humidified chamber at 37 °C, under an atmosphere containing 5 % CO₂.

Gene expression profiling and methylation analysis

Total RNA and DNA were extracted with NucleoSpin RNAII and NucleoSpin Tissue kits, respectively (Macherey–Nagel, Hoerd, France). Gene expression profiling was performed with the Agilent Whole Human Genome 8 × 60 K Microarray Kit (Agilent Technologies, Santa Clara, USA) and DNA methylation profiling was performed with the Infinium Human Methylation 450 bead-chip (Illumina Inc., San Diego, USA). For a detailed description of the gene expression profiling and methylation analysis, see Supplementary Methods.

Phenotypic analysis by flow cytometry

The following primary antibodies were used for flow cytometry: anti-CD146/MCAM, anti-PDGFRβ/CD140b, anti-ICAM1, anti-EGFR and isotype control antibodies from BD Biosciences (Le Pont de Claix, France); anti-αSMA, anti-nestin and anti-NG2/CSPG4 antibodies from R&D Systems (Lille, France); and anti-S100A4/FSP1, anti-THBS1 and anti-VASP antibodies from Abcam (Paris, France). The staining protocol used was as previously described [7, 8]. The stained cells were analyzed in a FACScan flow cytometer with Cell Quest Software (BD Biosciences).

Preparation of conditioned media

GASCs were grown to 70–80 % confluence in DMEM-HG containing 10 % HABS and 1 % antibiotics. The medium was replaced with EBM-2 or DMEM-HG supplemented with 0.1 % HSA and 0.2 % antibiotics and the cells were cultured for a further 24 h. The resulting conditioned medium (CM) was centrifuged and stored at –20 °C for subsequent use.

Functional analyses on GB cell lines

Invasion assay

Transwell inserts (Millicell® cell culture inserts, 8 μm pore size) with a thin layer of Matrigel basement membrane matrix (BD Biosciences) were used to assess A172 cell invasion in response to factors secreted by GASCs. Briefly, A172 cells (5 × 10⁴ cells) were added to the upper chamber, and 500 μl of negative control medium (DMEM-HG supplemented with 0.1 % HSA and 0.2 % antibiotics), positive control medium (10 % HABS) or GASC-CM was

added to the bottom chamber. After 6 h, the cells that had invaded to the underside of the insert membrane were stained with hematoxylin and counted with a computerized image-analysis system (MetaView, Roper Scientific, Evry, France). Six fields per insert, at a magnification of ×200, were used to count the cells that had invaded. Cell invasion values are expressed as mean ± SEM of the percentage of cells invading in the different conditions.

In vitro proliferation assay

We assessed the ability of GASCs to affect the proliferation of GB cells, using the aneuploid glioma cell line A172, to make it possible to distinguish between tumor cells and diploid GASCs. GASCs were used to seed six-well plates, at a density of 96 × 10³ cells per well, and were cultured in DMEM supplemented with 10 % HABS and 1 % antibiotics for 24 h. We then added 96 × 10³ A172 cells per well. The cells were cocultured for 3 days and then harvested. We used Vindelov's protocol to stain chromosomal DNA [9] and the cells were analyzed by flow cytometry with a FACScan flow cytometer (BD Biosciences). We calculated the DNA index (DI) and the percentages of the cell populations in each culture, as determined on the basis of their DNA content, with Modfit version 5.2 software (Verity Software House, Topsham, Maine), as previously described [10]. Cell-cycle analysis was carried out on the aneuploid A172 cells, and the proliferation index (PI) of these cells was evaluated as the percentage of cells in S+G2M phase.

In vivo implantation

Female Swiss nude mice (8–10 weeks old) were obtained from Charles River Laboratories (L'Arbresle, France). The protocol was approved by the Committee on the Ethics of Animal Experiments of the "Pays de la Loire" (Permit Number: CEEA.2010.45). U87MG cells were subcutaneously injected into the right flank alone (0.5 × 10⁶ cells, n = 7) or together with 0.5 × 10⁶ GASCs [GASC-A (GASC-31); n = 5 or GASC-B (GASC-3); n = 4]. Tumor volume within the flank was determined by direct measurement with a digital caliper, twice weekly, and was calculated as follows:

$$0.5 \times (\text{largest diameter}) \times (\text{smallest diameter})^2.$$

The results are expressed as median ± SEM.

Functional analyses on HUVECs

Migration assay

Transwell inserts (Millicell® cell culture inserts, 8 μm pore size, Millipore) were used to assess the migration of

HUVECs in response to factors secreted by GASCs. For these experiments, HUVECs (2.5×10^4 cells) were added to the upper chamber, and 500 μ l of negative control medium (EBM-2 with 0.1 % HSA and 0.2 % antibiotics), positive control medium [10 % foetal calf serum (FCS)] or GASC-CM was added to the bottom chamber. After 6 h, the cells that had migrated to the underside of the insert membrane were stained and counted with a computerized image-analysis system, as described above.

Proliferation assay

HUVECs (1×10^4 cells/cm²) were plated in 96-well plates. They were incubated for 48 h, after which, the culture medium was replaced with 100 μ l of negative control medium (EBM-2 supplemented with 0.1 % HSA and 0.2 % antibiotics), positive control medium (EGM-2) or GASC-CM. The plate was incubated for 72 h. The medium was then removed from the wells and the plate was stored at -80°C until the assay was carried out. Cell survival was estimated with the CyQUANT[®] cell proliferation assay kit, according to the manufacturer's instructions (Fisher Scientific, Illkirch, France). Sample fluorescence was measured with a microplate reader (Fluoroskan Ascent FL, Labsystem, Cergy-Pontoise, France). The fluorescence of HUVECs incubated with the negative control medium was considered to correspond to 100 % survival.

Endothelial tubule formation

HUVECs (5×10^4 cells/cm²) were used to seed 96-well plates coated with Matrigel basement membrane matrix (50 μ l/well, BD Biosciences), and were incubated for 6 h in EBM-2 negative control medium, EGM-2 positive control medium or GASC-CM. The length of the endothelial tubule in each field was quantified with Image J software. Data are expressed as mean \pm SEM.

Statistical analysis

Results are expressed as mean \pm SEM. The Kruskal–Wallis test was used for statistical analyses. Differences were considered significant if $P < 0.05$.

Results

Gene expression profiles identify two subgroups of GASCs derived from GB

We performed an unsupervised hierarchical clustering analysis to group samples according to their transcriptomic

profiles (4,122 selected probes with an SD ≥ 0.5). The results of the clustering analysis are presented in the dendrogram in Fig. 1a. We observed that the samples clustered into two main groups: group A, corresponding to four GASC samples and three control stromal cell samples derived from two patients with epilepsy and one patient with an epidermoid cyst, and group B, corresponding to 10 GASC samples and two control stromal cell samples derived from a patient with meningioma and a patient with craniopharyngioma (Fig. 1a). Genome-wide methylation profiling gave the same clustering pattern (Fig. 1b). Given the heterogeneity of the control stromal cells, we decided to limit our comparisons to group A GASCs (GASC-A) and group B GASCs (GASC-B) in this study.

Genes differentially expressed between GASC-A and GASC-B

We found that 895 (713 genes) of the 4,122 selected probes were differentially expressed between GASC-A and GASC-B: 422 probes (339 genes) were overexpressed and 473 probes (374 genes) were underexpressed in GASC-B (Supplementary Table 2). As expected, hierarchical cluster analysis of the 895 differentially expressed probes clustered GASC samples into GASC-A and GASC-B groups (data not shown). Functional annotation of the differentially expressed genes (NIH-David software) showed enrichment in several Gene Ontology biological processes (Fisher's exact test): cell division, nervous system development, blood vessel development, inflammatory response, epidermal growth factor receptor signaling pathway, cell motion and muscle system processes (Table 1).

We found that 80 of the 339 (24 %) overexpressed genes were hypomethylated in GASC-B and 85 of the 374 (23 %) underexpressed genes were hypermethylated in GASC-B (Supplementary Table 2). The differentially methylated genes corresponding to the biological term enrichments described above are indicated in Table 1.

Validation of transcriptomic data for the selected genes

The differential expression of six genes was confirmed by flow cytometry analyses: GASC-B overexpressed VASP, nestin, THBS1 and CSPG4/NG2 and underexpressed EGFR and ICAM1 (Fig. 2). We also found that the expression of other myofibroblast- or CAF-associated markers, including α SMA, PDGFR β /CD140b and S100A4/FSP1, was stronger in GASC-B than in GASC-A (Fig. 2). These markers were previously shown to be more strongly expressed in GASCs than in control stromal cells [7].

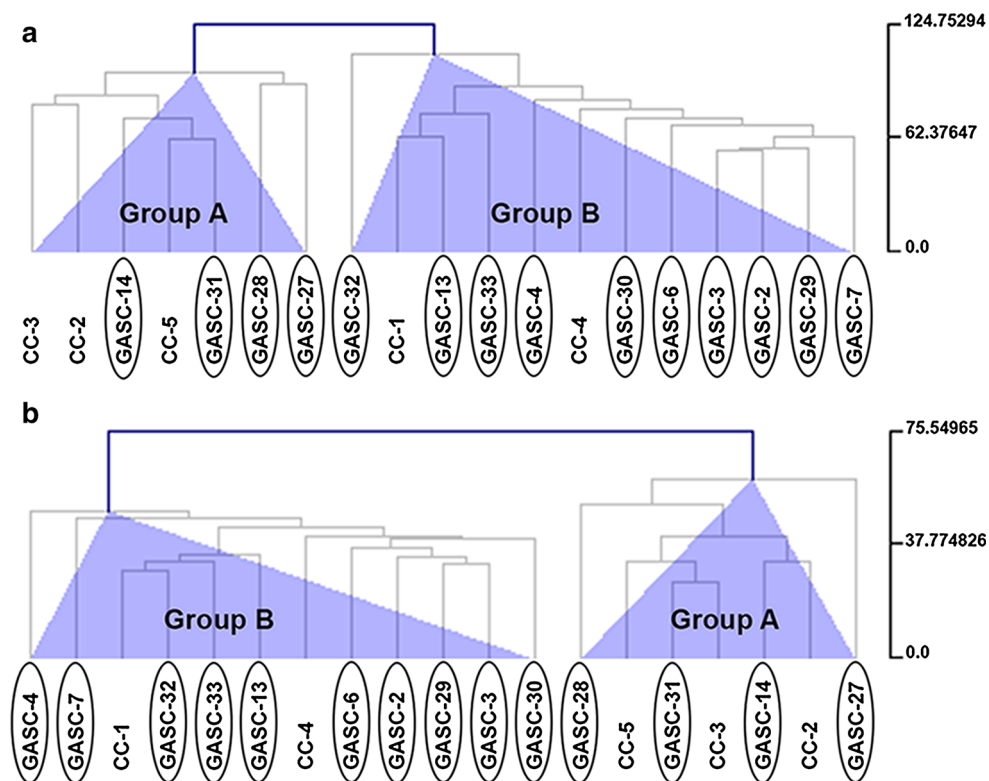


Fig. 1 Hierarchical clustering dendrograms showing gene expression (a) and DNA methylation (b) data from GASCs and control stromal cells. In the dendrogram, the samples or groups (clusters) of samples with similar expression patterns are linked by branches. The vertical axis of the dendrogram represents the distance (dissimilarity) between samples or clusters of samples. The length of the each branch is correlated with size of the difference between the samples it connects.

Two main clusters of samples are observed: group A, corresponding to four GASC samples and three control stromal cell samples derived from two patients with epilepsy and one patient with an epidermoid cyst, and group B, corresponding to ten GASC samples and two control stromal cell samples derived from a patient with meningioma and a patient with craniopharyngioma

Tumor-promoting properties of the two subgroups of GASCs

We investigated whether the two subtypes of GASCs identified by transcriptome analysis were associated with different tumor-promoting properties, such as invasion and proliferation, using the aneuploid A172 GB cell line. GASC-CM resulted in a greater invasion capacity of A172 cells than culture in the positive control medium (10 % HABS) (Fig. 3a). No significant difference was observed between the two subgroups of GASCs. No invasion by A172 cells was observed in the presence of the negative control medium (data not shown). The addition of GASC-B to the aneuploid A172 cell line induced an increase in tumor cell proliferation, which was significantly stronger than after the addition of GASC-A (Fig. 3b). This result was validated in vivo, with the diploid tumorigenic U87MG cell line. The subcutaneous injection into nude mice of GASC-B together with the U87MG cell line resulted in a significantly higher tumor volume induction than the injection of U87MG cells, either alone or in together with GASC-A (Fig. 3c).

Endothelium-promoting abilities of the two subgroups of GASCs

We assessed the effect of the two subgroups of GASCs on the migration, proliferation and tubule formation of endothelial cells (Fig. 4). We found that both subgroups of GASCs induced slightly higher levels of endothelial cell migration and proliferation than the negative control medium (Fig. 4a, b). No significant difference was observed between the two subgroups of GASCs. In tubule formation assays, GASC-B resulted in significantly longer tubules ($175.4 \pm 2.1 \mu\text{m}$) than GASC-A ($151.7 \pm 4.6 \mu\text{m}$) and the negative control medium ($158.7 \pm 4.9 \mu\text{m}$) (Fig. 4c, d).

Discussion

In this study, we identified two subtypes of GASCs in the histologically normal surgical margins of GB patients: GASC-A and GASC-B. The genes differentially expressed between the two subtypes were significantly associated

Table 1 GO biological process enrichment of the genes differentially expressed between GASC-A and GASC-B

	<i>P</i> value	Genes
GO:0051301_cell division	3.56×10^{-6}	CABLES1, C13ORF34, C14ORF106, CCNE2, CDK6, CDKN2A, CENPH, CENPJ, CKS1B, ESPL1, FBXO5, HAUS8, HELLS, KIF20B, KNTC1, LIG1, MAD2L1, MCM5, NCAPD2, NCAPD3, NCAPG2, NEK1, NUF2, PARD3, PTTG1, PTTG2, RACGAP1, SKA3, SMC2, SMC4, ZWINT
GO:0007399_nervous system development	4.05×10^{-4}	<i>APOE</i> , ARNT2, BAI2, BAIAP2, BEX1 , C17ORF28, C1S, CABLES1, CDK5R1 , CDK6, CDKN1C, CLDN1, CLU, <i>CXCL1</i> , DCLK1, <i>DLC1</i> , DOK5, <i>EFHD1</i> , EFNB1, <i>EGFR</i> , EPOR , FEZ1, FGF5, GBX2 , GFRA1, <i>HEYL</i> , INA, <i>KCNMA1</i> , L1CAM , <i>LMO4</i> , MAFB, <i>MEF2C</i> , <i>MSX1</i> , NEFM, NES, NRGN, NTRK2, PARD3, <i>PBX1</i> , PHGDH, PLXNB1, PTK2B, PTN, RACGAP1 , RCAN2, RELN, RGS9, RTN1, RUNX3, SEMA5B , SEPP1, SERPINE2, <i>SERPINF1</i> , SLITRK4, SMAD1, TBX3 , TIAM1, TIMP3, TRIM3 , UCHL1, <i>VASP</i> , VLDLR, XRCC2, ZEB1, ZIC5
GO:0001568_blood vessel development	7.38×10^{-5}	ARHGAP22, APOE, CCBE1, CSPG4, EREG, FOXO1, GBX2, GJA4, GJCI , LAMA4, LMO2, LOX, NTRK2, PDGFA, PLCD3, PLXDC1, PLXND1 , PTK2B, RECK, <i>SEMA3C, TBX3, TGM2, THBS1, TIPARP</i>
GO:0006954_inflammatory response	0.026	AOC3, CIR , C1RL, C1S, C2, C4B, CD14, CD55, CDO1, CFB, CFD, CLU, <i>CXCL1, CYBA, IL17B, IL17D, IL20RB, NUPR1, S1PR3, SMAD1, THBS1</i>
GO:0007173_epidermal growth factor receptor signaling pathway	0.021	<i>EGFR, EREG, HBEGF</i> , PLCE1, PTK2B
GO:0051270_regulation of cell motion	0.003	<i>APOE, DLC1, EGFR</i> , ENPP2, HBEGF, ICAM1 , IGFBP3, IGFBP5, LAMA4, MYLK2 , PARD3, PDGFA , PTK2B, PTPRU, SERPINE2, THBS1 , TRIB1
GO:0003012_muscle system process	0.029	CYBA, GAA, GJCI, GUCY1A3, KCNMA1, MYH11, MYLK2, MYOM1, SCN5A, SLMAP, SMTN, TNNT2, VIPR1

Genes overexpressed in GASC-B are shown in bold. The remaining genes were underexpressed in GASC-B. Genes highlighted in italics correspond to genes overexpressed and hypomethylated in GASC-B or underexpressed and hypermethylated in GASC-B

Fig. 2 Phenotypic analysis by flow cytometry of GASC-A ($n = 4$) and GASC-B ($n = 4$). GASCs were immunostained with antibodies against CAF-associated markers (α SMA, CD140b, S100A4, CD146 and CSPG4), nestin, THBS1, VASP, EGFR and ICAM1. Results are expressed as mean \pm SEM of the fold-change ratio of the geometric mean marker/geometric mean isotype control and as mean \pm SEM of the difference between marker- and isotype control-positive cells ($*P < 0.05$ between GASC-A and GASC-B)

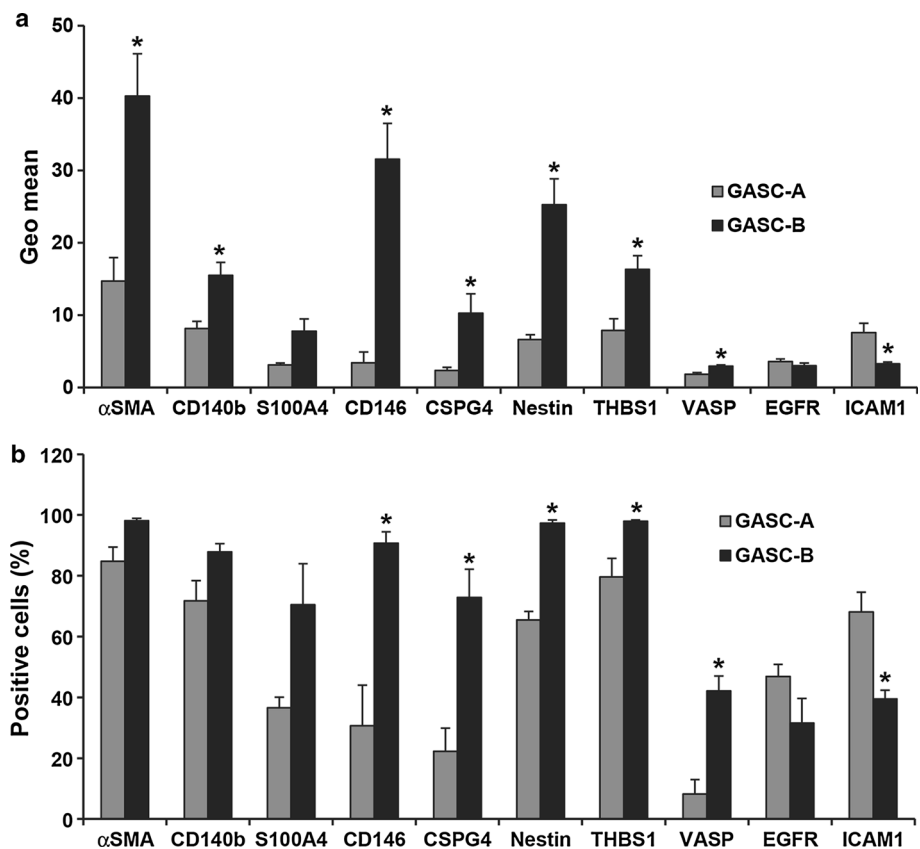
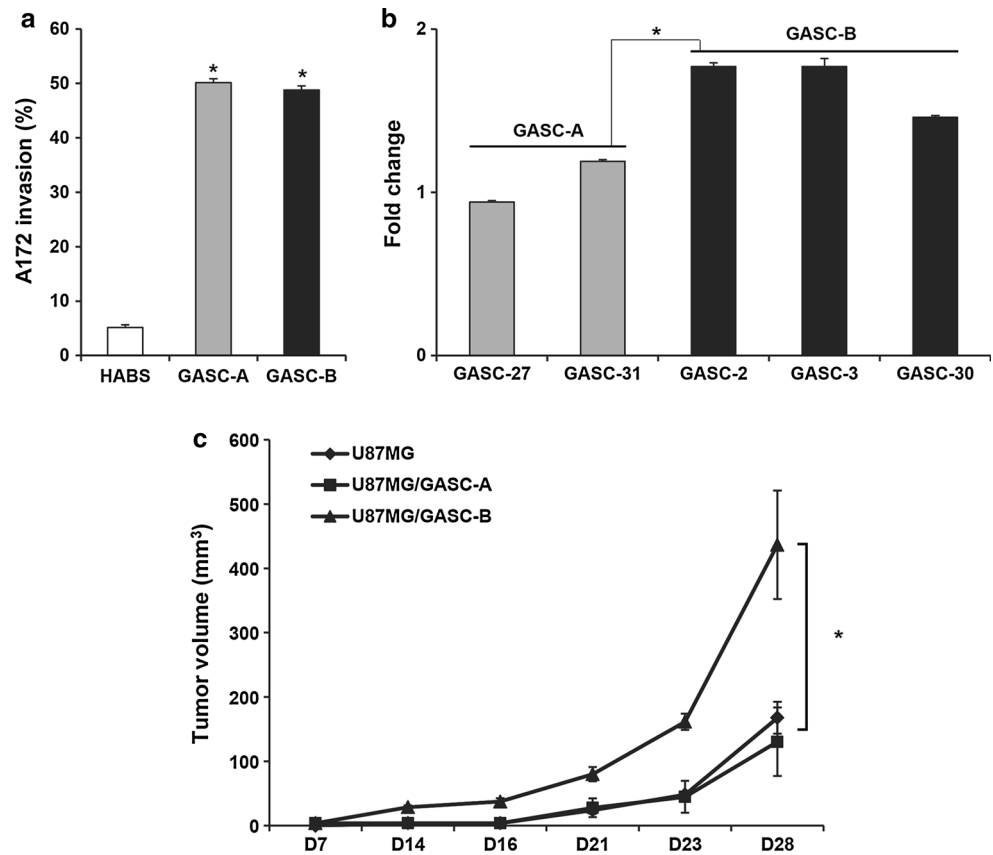


Fig. 3 **a** HABS or CM from GASC-A and GASC-B was added to the lower compartments of 24-well plates. A172 cells (5×10^4) were used to seed the Transwell inserts and the plates were incubated for 6 h. The percentage cells invading the lower compartment is presented (mean \pm SEM; $*P < 0.05$ vs HABS). **b** Direct coculture assay of GASC-A or GASC-B with the aneuploid glioma cell line A172. *Bar graphs* show mean \pm SEM of the PI fold-change between A172 cells cultured alone and A172 cells cocultured with GASCs ($*P = 0.001$ between GASC-A and GASC-B). **c** U87MG cells were injected alone ($n = 7$) or co-injected with GASC-A ($n = 5$) or GASC-B ($n = 4$) subcutaneously into nude mice. Tumor volume is plotted for the days indicated, as the median \pm SEM ($*P = 0.008$, vs U87MG alone)



with cell division, blood vessel development and muscle system processes. The GASC-B subtype, corresponding to 71 % of the GASC samples analyzed, displayed the characteristics of GASCs described in our previous studies [7]. This subtype had a myofibroblast phenotype and procarcinogenic properties. In particular, unlike the GASC-A subtype, it promoted GB cell growth in vitro and in vivo and increased the tube length of HUVECs, suggesting that it also had angiogenic properties. The GASC-B subtype did not appear to be specific to the GB microenvironment, as its transcriptome closely resembled those of control stromal cells derived from meningioma and craniopharyngioma. These CNS diseases are considered to display benign biological behavior, but they may present an infiltrative pattern and recur more frequently than other benign tumors [11, 12].

The cells of the GASC-B subtype overexpressed several markers, such as CSPG4/NG2, a transmembrane chondroitin sulfate, CD146/MCAM, a cell adhesion molecule, and nestin, a neural stem cell marker that we previously showed to be more strongly expressed in GASCs than in control stromal cells [7]. These molecules have been shown to be attractive potential biomarkers of cancer prognosis. For example, CSPG4/NG2 has been proposed as a prognostic marker for breast cancers [13], head and neck

squamous cell carcinomas (HNSCC) [14] and gliomas [15, 16]. The expression of nestin has been described in tumor and peritumor areas of GB, independently of the presence of neoplastic cells [17, 18]. Nestin expression has been shown to increase with malignancy grade, and high levels of nestin are associated with poor survival [19, 20]. CD146/MCAM is abnormally expressed in various tumors and is closely associated with tumor progression [21, 22]. CSPG4/NG2, nestin and CD146/MCAM are also potentially attractive targets for cancer treatment [21, 23, 24].

In this study, genome-wide methylation profiling and gene expression profiling gave the same clustering pattern, suggesting that the GASC-B phenotype may be partly driven by DNA methylation processes. Several studies have highlighted the importance of this epigenetic mechanism in the regulation of myofibroblast differentiation [25] and in the maintenance of CAF properties [26–29]. The genes differentially methylated between GASC-A and GASC-B included CSPG4/NG2 and CD146/MCAM, which were hypomethylated in GASC-B, resulting in their overexpression. Changes in the expression of CSPG4/NG2 due to hypomethylation have already been reported for the stroma of human colon carcinoma [30] and in HNSCC [14]. Conversely, ICAM-1 and EGFR were found to be hypermethylated in GASC-B, and this hypermethylation

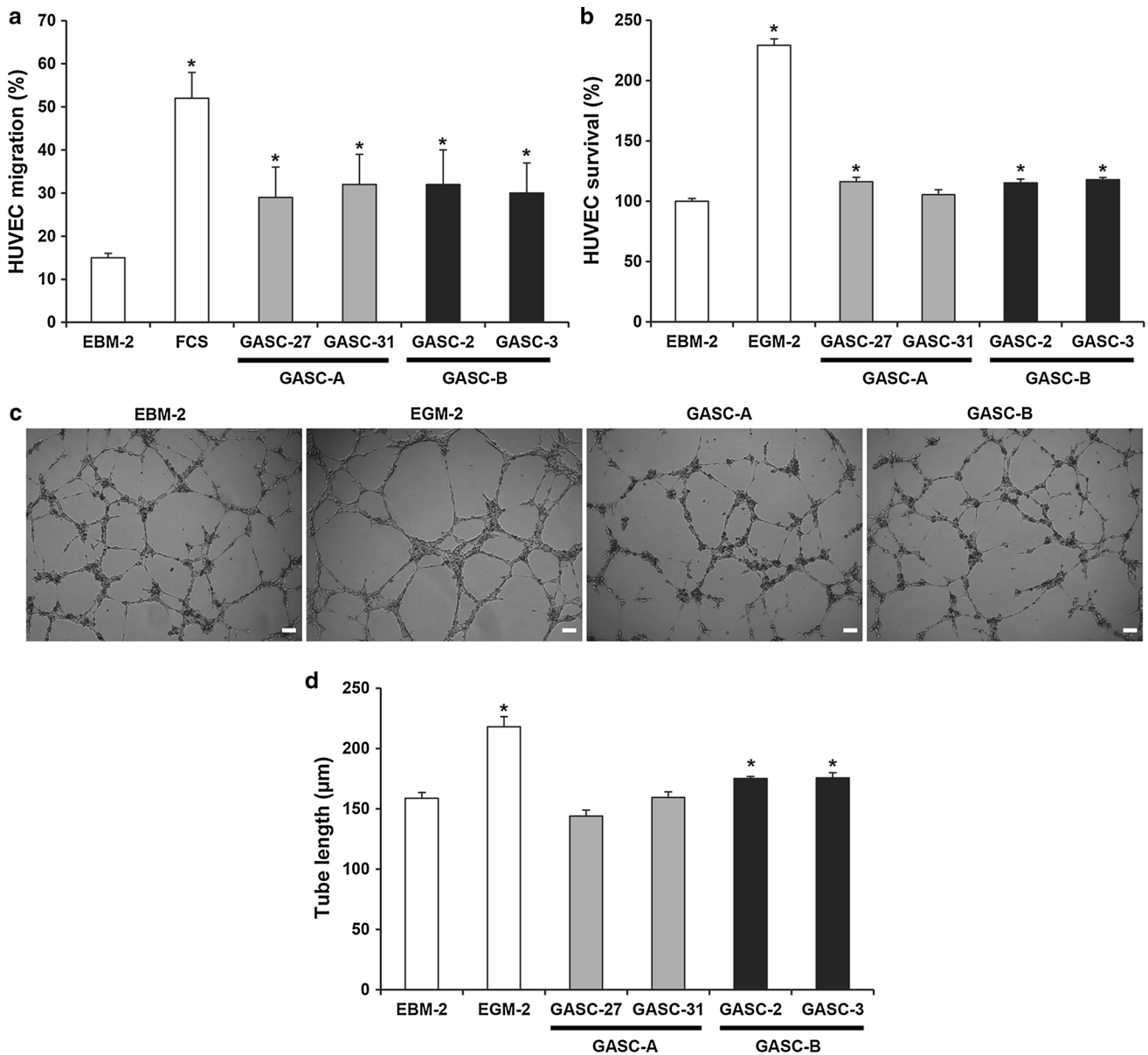


Fig. 4 **a** EBM-2, FCS or CM from GASC-A and GASC-B was added to the lower compartments of 24-well plates. HUVECs (2.5×10^4) were used to seed Transwell inserts and the plates were incubated for 6 h. The percentage of cells migrating is presented (mean \pm SEM; * $P < 0.05$ vs EBM-2). **b** Effect of GASCs on the survival of HUVECs. The cells were incubated for 3 days with EBM-2, EGM-2 or CM from GASC-A or GASC-B. The percentage of cells surviving

is presented (mean \pm SEM; * $P < 0.05$ vs EBM-2). **c**, **d** Effect of GASCs on tube length. **c** Phase-contrast micrographs of HUVEC tube formation on Matrigel. HUVECs were used to seed Matrigel and were incubated at 37 °C for 6 h in EBM-2, EGM-2 or CM from GASC-A or GASC-B (scale bar 100 μ m). **d** Tube length was used to quantify angiogenesis. Results are mean \pm SEM (* $P = 0.049$ vs EBM-2 or CM from GASC-A)

was associated with the underexpression of these genes. ICAM1 silencing by epigenetic regulation has been described in tumor endothelial cells, rendering these cells unresponsive to inflammatory activation [31]. EGFR hypermethylation has been described in a subset of tumors, including GB, breast, colon and lung cancers [32, 33], and may play a role in determining the efficacy of anti-EGFR treatments [33, 34]. In addition to DNA methylation, other mechanisms involved in myofibroblast differentiation,

including Wnt, Notch and hedgehog signaling, TGF- β and other types of epigenetic regulation, such as histone acetylation and/or small interfering RNAs [25], may induce the GASC-B phenotype.

Our findings indicate that two extratumoral microenvironments can be encountered in GB patients: an extratumoral microenvironment containing GASCs with procarcinogenic properties and another containing GASCs without such properties. In accordance with our findings,

Roman-Pérez et al. [35] reported the presence of two different subtypes of extratumoral microenvironment influencing the aggressiveness and outcome of human breast cancers. Furthermore, in 2013, Al Rakan et al. [36] carried out molecular and cellular characterizations of breast stromal fibroblasts (TCFs) from negative surgical margins. TCFs closely resemble GASCs in terms of their carcinogenic properties and patient-to-patient variability.

All these data indicate that the tumor microenvironment present after resection may play a determinant role in local recurrence. Consistent with this possibility, several studies have highlighted the importance of surgical margin status for determining the likelihood of local relapse [3, 37]. Pirrotte et al. [38] reported longer survival in patients undergoing complete resection of the area of increased tracer uptake on PET, whereas complete resection of the gadolinium-enhanced MR-delineated area did not affect survival, suggesting that metabolic PET may be a more useful presurgical imaging technique. Intraoperative tumor identification in fluorescence-guided surgery with 5-aminolevulinic acid (ALA) is also an emerging technique that increases the rate of complete resections and extends survival [39, 40]. In this era of personalized therapy, the characterization of tumor cells and the status of GASCs located in GB surgical margins should be taken into account, to improve the efficacy of treatment and the prevention of recurrence.

Acknowledgments We thank Abderrahmane Hamlat and Véronique Quillien (CHU, Rennes) for providing control and tumor samples. We also thank Pierre Legras and Jérôme Roux (Service Commun d'Animalerie Hospitalo-Universitaire, Angers), Catherine Guillet (Paltform PACeM, Angers), and the Cancéropole Grand Ouest for allowing us to use their facilities. We thank Alex Edelman and Associates for correcting the English language of the manuscript.

Conflict of interest We have no potential conflicts of interest to declare.

Funding This work was supported by the Pays de la Loire and Bretagne regions and Ligue contre le cancer-49-Comité de Maine-et-Loire.

References

- Stupp R, Mason WP, Van den Bent MJ et al (2005) Radiotherapy plus concomitant and adjuvant temozolomide for glioblastoma. *N Engl J Med* 352:987–996
- Stupp R, Hegi ME, Mason WP et al (2009) Effects of radiotherapy with concomitant and adjuvant temozolomide versus radiotherapy alone on survival in glioblastoma in a randomised phase III study: 5-year analysis of the EORTC-NCIC trial. *Lancet Oncol* 10:459–466
- Petrecca K, Guiot M-C, Panet-Raymond V, Souhami L (2013) Failure pattern following complete resection plus radiotherapy and temozolomide is at the resection margin in patients with glioblastoma. *J Neurooncol* 111:19–23
- Glas M, Rath BH, Simon M et al (2010) Residual tumor cells are unique cellular targets in glioblastoma. *Ann Neurol* 68:264–269
- Piccirillo SG, Dietz S, Madhu B, Griffiths J, Price SJ, Collins VP, Watts C (2012) Fluorescence-guided surgical sampling of glioblastoma identifies phenotypically distinct tumour-initiating cell populations in the tumour mass and margin. *Br J Cancer* 107:462–468
- Polanska UM, Orimo A (2013) Carcinoma-associated fibroblasts: non-neoplastic tumour-promoting mesenchymal cells. *J Cell Physiol* 228:1651–1657
- Clavreul A, Guette C, Faguer R et al (2014) Glioblastoma-associated stromal cells (GASCs) from histologically normal surgical margins have a myofibroblast phenotype and angiogenic properties. *J Pathol* 233:74–88
- Clavreul A, Etchevery A, Chassevent A et al (2012) Isolation of a new cell population in the glioblastoma microenvironment. *J Neurooncol* 106:493–504
- Vindelov LL, Christensen IJ, Nissen NI (1983) A detergent-trypsin method for the preparation of nuclei for flow cytometric DNA analysis. *Cytometry* 3:323–327
- Clavreul A, Jean I, Preisser L, Chassevent A, Sapin A, Michalak S, Menei P (2009) Human glioma cell culture: two FCS-free media could be recommended for clinical use in immunotherapy. *In Vitro Cell Dev Biol Anim* 45:500–511
- Prieto R, Pascual JM, Subhi-Issa I, Jorquera M, Yus M, Martínez R (2013) Predictive factors for craniopharyngioma recurrence: a systematic review and illustrative case report of a rapid recurrence. *World Neurosurg* 79:733–749
- Abdelzaher E, El-Gendi SM, Yehya A, Gowil AG (2011) Recurrence of benign meningiomas: predictive value of proliferative index, BCL2, p53, hormonal receptors and HER2 expression. *Br J Neurosurg* 25:707–713
- Hsu NC, Nien P-Y, Yokoyama KK, Chu P-Y, Hou M-F (2013) High chondroitin sulfate proteoglycan 4 expression correlates with poor outcome in patients with breast cancer. *Biochem Biophys Res Commun* 441:514–518
- Warta R, Herold-Mende C, Chaisaingmongkol J et al (2014) Reduced promoter methylation and increased expression of CSPG4 negatively influences survival of HNSCC patients. *Int J Cancer*. doi:10.1002/ijc.28906
- Svensden A, Verhoeff JJC, Immervoll H et al (2011) Expression of the progenitor marker NG2/CSPG4 predicts poor survival and resistance to ionising radiation in glioblastoma. *Acta Neuropathol* 122:495–510
- Chekenya M, Pilkington GJ (2002) NG2 precursor cells in neoplasia: functional, histogenesis and therapeutic implications for malignant brain tumours. *J Neurocytol* 31:507–521
- Mangiola A, Lama G, Giannitelli C et al (2007) Stem cell marker nestin and c-Jun NH2-terminal kinases in tumor and peritumor areas of glioblastoma multiforme: possible prognostic implications. *Clin Cancer Res* 13:6970–6977
- Sica G, Lama G, Anile C, Geloso MC, La Torre G, De Bonis P, Maira G, Lauriola L, Jhanwar-Uniyal M, Mangiola A (2011) Assessment of angiogenesis by CD105 and nestin expression in peritumor tissue of glioblastoma. *Int J Oncol* 38:41–49
- Dahlrot RH, Hermansen SK, Hansen S, Kristensen BW (2013) What is the clinical value of cancer stem cell markers in gliomas? *Int J Clin Exp Pathol* 6:334–348
- Hatanpaa KJ, Hu T, Vemireddy V et al (2014) High expression of the stem cell marker nestin is an adverse prognostic factor in WHO grade II-III astrocytomas and oligoastrocytomas. *J Neurooncol* 117:183–189
- Wang Z, Yan X (2013) CD146, a multi-functional molecule beyond adhesion. *Cancer Lett* 330:150–162

22. Kapoor S (2013) CD146 expression and its close relationship to tumor progression in systemic malignancies besides gall bladder carcinomas. *Tumour Biol* 34:1273–1274
23. Wang J, Svendsen A, Kmiecik J et al (2011) Targeting the NG2/CSPG4 proteoglycan retards tumour growth and angiogenesis in preclinical models of GBM and melanoma. *PLoS One* 6:e23062
24. Matsuda Y, Hagio M, Ishiwata T (2013) Nestin: a novel angiogenesis marker and possible target for tumor angiogenesis. *World J Gastroenterol* 19:42–48
25. Hu B, Phan SH (2013) Myofibroblasts. *Curr Opin Rheumatol* 25:71–77
26. Hu M, Yao J, Cai L, Bachman KE, Van den Brûle F, Velculescu V, Polyak K (2005) Distinct epigenetic changes in the stromal cells of breast cancers. *Nat Genet* 37:899–905
27. Hanson JA, Gillespie JW, Grover A, Tangrea MA, Chuaqui RF, Emmert-Buck MR, Tangrea JA, Libutti SK, Linehan WM, Woodson KG (2006) Gene promoter methylation in prostate tumor-associated stromal cells. *J Natl Cancer Inst* 98:255–261
28. Jiang L, Gonda TA, Gamble MV et al (2008) Global hypomethylation of genomic DNA in cancer-associated myofibroblasts. *Cancer Res* 68:9900–9908
29. Tyan S-W, Hsu C-H, Peng K-L, Chen C-C, Kuo W-H, Lee EY-HP, Shew J-Y, Chang K-J, Juan L-J, Lee W-H (2012) Breast cancer cells induce stromal fibroblasts to secrete ADAMTS1 for cancer invasion through an epigenetic change. *PLoS One* 7:e35128
30. Adany R, Heimer R, Catterson B, Sorrell JM, Iozzo RV (1990) Altered expression of chondroitin sulfate proteoglycan in the stroma of human colon carcinoma. Hypomethylation of PG-40 gene correlates with increased PG-40 content and mRNA levels. *J Biol Chem* 265:11389–11396
31. Hellebrekers DMEI, Castermans K, Viré E et al (2006) Epigenetic regulation of tumor endothelial cell anergy: silencing of intercellular adhesion molecule-1 by histone modifications. *Cancer Res* 66:10770–10777
32. Gömöri E, Pál J, Kovács B, Dóczy T (2012) Concurrent hypermethylation of DNMT1, MGMT and EGFR genes in progression of gliomas. *Diagn Pathol* 7:8
33. Montero AJ, Díaz-Montero CM, Mao L, Youssef EM, Estecio M, Shen L, Issa J-PJ (2006) Epigenetic inactivation of EGFR by CpG island hypermethylation in cancer. *Cancer Biol Ther* 5:1494–1501
34. Scartozzi M, Bearzi I, Mandolesi A et al (2011) Epidermal growth factor receptor (EGFR) gene promoter methylation and cetuximab treatment in colorectal cancer patients. *Br J Cancer* 104:1786–1790
35. Román-Pérez E, Casbas-Hernández P, Pirone JR, Rein J, Carey LA, Lubet RA, Mani SA, Amos KD, Troester MA (2012) Gene expression in extratumoral microenvironment predicts clinical outcome in breast cancer patients. *Breast Cancer Res* 14:R51
36. Al-Rakan MA, Colak D, Hendrayani S-F, Al-Bakheet A, Al-Mohanna FH, Kaya N, Al-Malik O, Aboussekhra A (2013) Breast stromal fibroblasts from histologically normal surgical margins are pro-carcinogenic. *J Pathol* 231:457–465
37. De Bonis P, Anile C, Pompucci A, Fiorentino A, Balducci M, Chiesa S, Lauriola L, Maira G, Mangiola A (2013) The influence of surgery on recurrence pattern of glioblastoma. *Clin Neurol Neurosurg* 115:37–43
38. Pirotte BJM, Levivier M, Goldman S, Massager N, Wikler D, Dewitte O, Bruneau M, Rorive S, David P, Brotchi J (2009) Positron emission tomography-guided volumetric resection of supratentorial high-grade gliomas: a survival analysis in 66 consecutive patients. *Neurosurgery* 64:471–481
39. Stummer W, Pichlmeier U, Meinel T, Wiestler OD, Zanella F, Reulen H-J (2006) Fluorescence-guided surgery with 5-aminolevulinic acid for resection of malignant glioma: a randomised controlled multicentre phase III trial. *Lancet Oncol* 7:392–401
40. Aldave G, Tejada S, Pay E, Marigil M, Bejarano B, Idoate MA, Díez-Valle R (2013) Prognostic value of residual fluorescent tissue in glioblastoma patients after gross total resection in 5-aminolevulinic acid-guided surgery. *Neurosurgery* 72:915–920